Investigation of X-Ray Plasmon Scattering in Single-Crystal Beryllium

P. Eisenberger, P. M. Platzman, and K. C. Pandy*
Bell Laboratories, Murray Hill, New Jersey 07974
(Received 4 May 1973)

X-ray scattering studies in single-crystal beryllium reveal for the first time an anisotropy in both the plasmon dispersion and linewidth. By comparing the data with random-phase-approximation–type theory which includes band structure, we can begin to separate the contributions from the lattice and from the true many-body interactions to the temporally and spatially dependent response of an interacting electron gas at metallic densities.

Understanding the frequency- and wave-vector-dependent response function of a strongly correlated electron liquid at metallic densities is one of the most important and interesting problems in many-body physics. While there has been some experimental investigation of plasmons in beryllium by both electron[1,2] and x-ray[3-5] scattering with the results interpreted on the basis of the Bohm-Pines electron gas theory,[6] none of these studies, nor plasmon studies on the other materials, has been performed on single crystals. The absence until now of single-crystal measurements has prevented one from quantitatively assessing the relative contributions of the lattice interactions and the true many-body interactions.

The observed anisotropies arise from the interactions of the electrons with the lattice. Using a weak-coupling random-phase-approximation (RPA)–type theory we will show how such anisotropies can occur.[7] Even though quantitative agreement with the observed anisotropies has not been obtained, we can certainly assert that for electrons in metallic systems the interaction with the lattice produces effects on dispersion and lifetimes which are much larger than many of the refinements to RPA that have been previously calculated. Furthermore, the data obtained here for momentum transfer $k \simeq k_F$ seem to suggest a breakdown of an RPA-type treatment. In fact a major conclusion of this work is that studies such as this one in different metals with quantitatively different band structures should provide information on the behavior of the interacting conduction-electron liquid.

In this work we make use of the x-ray flux from a new x-ray source (60 kV, 1000 mA) to study the plasmons in single-crystal Be with good statistics and high resolution. Our study spans the momentum-transfer region 0.64 to 1.55 Å^{-1} with the momentum transfer along the C or A axis in hcp Be. We find that the plasmon dispersion is different in the two directions. Thus, even though the $k = 0$ plasmon frequencies are nearly identical, at momentum transfers of ~1 Å^{-1} they differ in the two directions by 1 eV or ~5% with that along the C axis being higher. In addition we observe that the widths and the shapes of the plasmon peaks differ with the general feature that the plasmon peak along the C axis is narrower.

The experimental setup is similar to that used by other investigators[8] except that in this study Ge(220) crystals (0.75-eV energy resolution) were used to analyze the energy of the radiation scattered at a scattering angle fixed by slits to $\pm\frac{1}{2}°$. Copper x-rays, $K\alpha_1$ and $K\alpha_2$, with about 2.5- and 3.5-eV natural linewidths and separated by 19.95 eV, were the source of radiation. At each scattering angle the energy of the radiation was analyzed by a double Bragg spectrometer in a 100-eV region around the $K\alpha_1$ and $K\alpha_2$ lines. In Fig. 1(a) we show the response of the system to a sample which scatters only elastically (thermal diffuse) the $K\alpha_1$ and $K\alpha_2$ x rays. In Fig. 1(b) is displayed the spectrum observed at the same scattering angle but with the Be sample in the beam. The spectrum in Fig. 1(a) was used in a trial-and-error technique to remove the elastically scattered x rays from the spectrum in Fig. 1(b) with the results shown in Fig. 1(c). Making use of the known $K\alpha_1$ and $K\alpha_2$ separation and linewidths we were able to calibrate the spectrometer (relate angle to energy).

The x-ray scattering cross section is given by[7]

$$\frac{d^2\sigma}{d\Omega\, d\omega} = (\vec{\epsilon}_1 \cdot \vec{\epsilon}_2)^2 \left(\frac{e^2}{mc^2}\right)^2 \left(\frac{k^2}{4\pi}\right) \mathrm{Im}\left(\frac{1}{\epsilon(\vec{k}, \omega)}\right). \quad (1)$$

Here,

$$[\epsilon(\vec{k}, \omega)]^{-1} = \left[1 - \frac{4\pi}{(\vec{k}+\vec{G})^2}\alpha(\vec{k}+\vec{G}, \vec{k}+\vec{G}', \omega)\right]^{-1}, \quad (2)$$

where α is the polarizability tensor (in recipro-

cal lattice vectors $\vec{G}$) of the electrons. In the mean-field or RPA approximation α is replaced by α^0, the polarizability for an inhomogeneous but noninteracting electron gas, i.e.,

$$\alpha^0(\vec{k}+\vec{G}, \vec{k}+\vec{G}', \omega) = \sum_{\vec{p}, ll'} \frac{[n(l,\vec{p}) - n(l',\vec{p}+\vec{k})]\langle l,\vec{p}|e^{-i(\vec{k}+\vec{G})\cdot\vec{r}}|l',\vec{p}+\vec{k}\rangle\langle l',\vec{p}+\vec{k}|e^{i(\vec{k}+\vec{G}')\cdot\vec{r}}|l,\vec{p}\rangle}{[\omega + E(l,\vec{p}) - E(l',\vec{p}+\vec{k}) + i\delta]}. \quad (3)$$

Here l and $\vec{p}$ label the energy band and crystal momentum, and $E(l,\vec{p})$ and $n(l,\vec{p})$ are the energy and occupation number of these states.

In the homogeneous case the tensor α^0 is diagonal, and the peaklike structure in the scattering spectrum at small momentum transfer arises from the zeros of ϵ, i.e., the plasmons. At scattering angles larger than a critical value, even in this homogeneous case, the dielectric constant becomes complex; the plasmon couples to the single-particle modes and is damped. The spectrum smears out, evolving at higher momentum transfers into a Compton-like spectrum.

One-electron band structure introduces several additional effects. At long wavelengths the plasmon is no longer well defined but may decay by virtue of umklapp processes to real electron-hole pairs in different bands. The off-diagonal components of the tensor characterize the coupling of a density fluctuation at $\vec{k}$ to ones at $\vec{k}+\vec{G}$. They lead to the banding of the plasmon and the

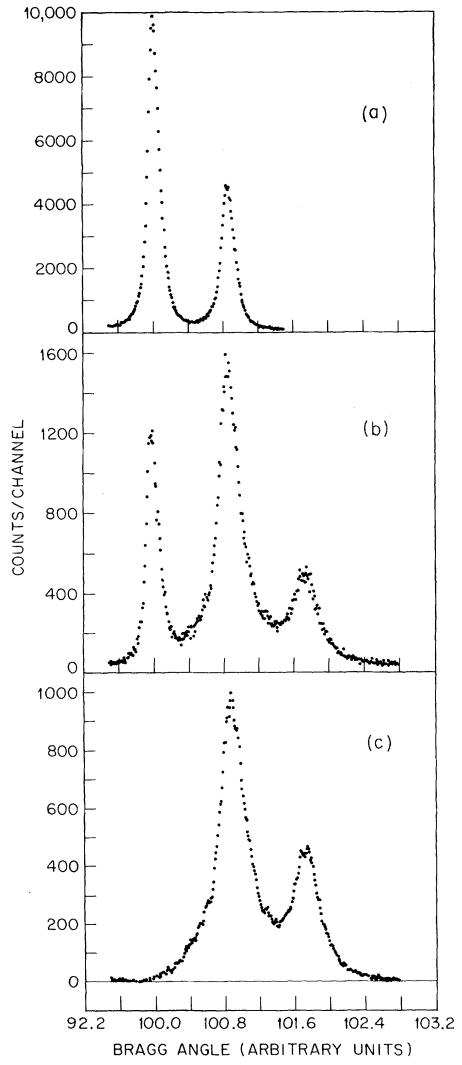

FIG. 1. Spectra obtained by sweeping double-crystal spectrometer. Two points are separated by 0.235 eV. (a) Elastically scattered Cu $K\alpha_1, K\alpha_2$ x rays. (b) Be [k =1 Å^{-1}, $\vec{k} \| C$]. (c) Be spectrum after removal of elastic components. Plasmon loss lines from $K\alpha_1$ and $K\alpha_2$ input remain.

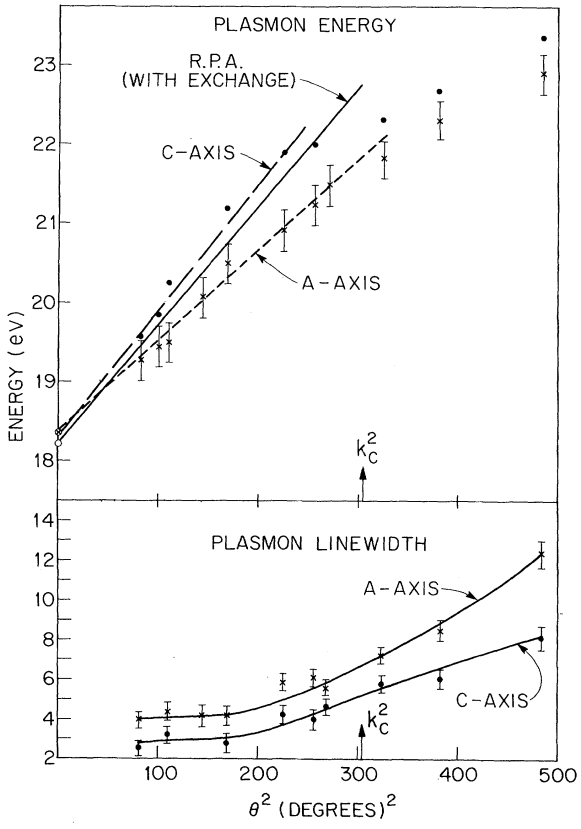

FIG. 2. Plasmon energy and linewidth for $\vec{k} \| C$ (circles) and $\vec{k} \| A$ (crosses) as a function of the square of the scattering angle (θ). The error bars on the C-axis dispersion data are the same as the A axis. The linewidth is the full width at half-maximum. As $|k|$ increases the observed line shapes are not simple, and so the energy position of the peak must be used with caution.

existence at $\vec{k}=0$ of higher-order plasmon bands.

The behavior of Eqs. (1)–(3) depends on the details of the band structure and may be quite complex. In order to understand the physical role of these effects and to get a quantitative estimate of them for Be, we have evaluated $\alpha^0(\vec{k}+\vec{G}, \vec{k}+\vec{G}, \omega)$ at high frequencies and used this expansion to analyze the x-ray data. More detailed calculations show this to be a valid procedure in Be where the plasma energy is at about 20 eV, a high energy relative to typical interband energies.

Using commutator techniques[7] to perform the intermediate-state sums present in α^0, we find to order ω^{-4} in the diagonal terms and ω^{-2} in the off-diagonal term ($m=\hbar=1$)

$$\alpha^0(\vec{k}+\vec{K}, \vec{k}+\vec{K}, \omega)=\frac{q^2N}{\omega^2}-\frac{1}{\omega^4}\sum_{\vec{G}}(\vec{q}\cdot\vec{G})^2V_{\vec{G}}\rho_{\vec{G}}-\frac{3q^2}{\omega^4}\sum_{l,\vec{p}}n(l,\vec{p})\langle l,\vec{p}|(\vec{q}\cdot\vec{\nabla})^2|l,\vec{p}\rangle+\frac{q^6N}{4\omega^4},$$
$$\alpha^0(\vec{k}+\vec{K}, \vec{k}+\vec{K}', \omega)=\frac{(\vec{k}+\vec{K})\cdot(\vec{k}+\vec{K}')}{\omega^2}\rho(\vec{K}'-\vec{K}), \tag{4}$$

where $\vec{q}=\vec{k}+\vec{K}$, N is the average electron density, and $V_{\vec{G}}$ and $\rho_{\vec{G}}$ are the $\vec{G}$th Fourier component of the lattice potential (including the structure factor) and the electron density. We observe from Eq. (4) the following:

(1) The leading diagonal term gives the free-electron plasmon frequency.

(2) The next term in ω^{-4} modifies the position of the zero–wave-vector plasmon. In a hexagonal crystal it is generally anisotropic, while in a cubic material it is isotropic. It represents the effects of interband transition on the plasmon.[9] Since the plasmon is assumed to be at high frequencies relative to the interband transitions, the sign of this term is such as to push the plasmon *up* in frequency.

(3) The next term characterizes the k^2 dispersion of the plasmon. In the absence of band-structure effects it gives the usual dispersion $\omega_p^2(k)=\omega_p^2(0)+\frac{3}{5}k^2v_F^2$. In general it will give rise to an anisotropy in the plasmon dispersion.

(4) The off-diagonal term comes in squared when one inverts the tensor given in Eq. (2). It is of such a sign as to decrease the frequency of the long-wavelength plasmon, i.e., the higher plasmon bands push *down* the lowest branch of the spectrum.

(5) This high-frequency limit completely omits linewidth effects.

The compiled experimental results are plotted in Fig. 2. The arrow on the scattering-angle axis (momentum transfer squared) indicates the position of the RPA cutoff momentum ($k_c=\omega_p/v_F=1.24$ Å^{-1}). The dispersion data are consistent with an intercept at $k=0$ for both C and A axes of 18.35 $\pm$ 0.35 eV and a dispersion which is about 30% different in the two directions. The linewidth data show the plasmon to be considerably narrower along the C axis with an experimental width (after removal of resolution effects) at $k=0$ of about 3 eV along C and 5 eV along A. The long-wavelength limit of the plasmon dispersion relation for the high-density homogeneous gas (including exchange)[7] is shown in Fig. 2(a). The intercept at $k=0$ (18.2 eV) is within experimental error of the observed value at 18.35 eV. The slope, which has about a 10% exchange softening in it, agrees with the experimental C-axis slope. The theoretical linewidth prediction[10] for the homogeneous electron gas originating from two pair final states is not plotted since it gives a linewidth of 0.25 eV at $k/k_c=1$ for Be. This width is a factor of 25 smaller than the observed value.

We have attempted to evaluate Eq. (4) to predict quantitatively the observed features of the spectrum. The crossed circle at $k=0$ in Fig. 2 corresponds to a computed value using Eq. (4) and a weak pseudopotential[11] model for the band structure. A similar evaluation for the dispersion corrections due to band structure yields results which (for suitable choice of the pseudopotential parameters) are anisotropic in qualitatively the correct way, but almost an order of magnitude too small to account for the data. Using Eq. (4) we have also estimated the importance of core orthogonalization effects on this dispersion term, and find these effects to be 2 orders of magnitude smaller than the observed anisotropy.

At the largest scattering angles studied, the spectrum has a rather peculiar and not understood shape. The two crystal directions for this 22° ($k=1.55$ Å^{-1}) scattering angle are shown in Fig. 3 along with a plot of the homogeneous RPA result[12] after it has been convoluted with the experimental resolution function. The two experimental spectra are centered at nearly the same energy but have different shapes. They both in

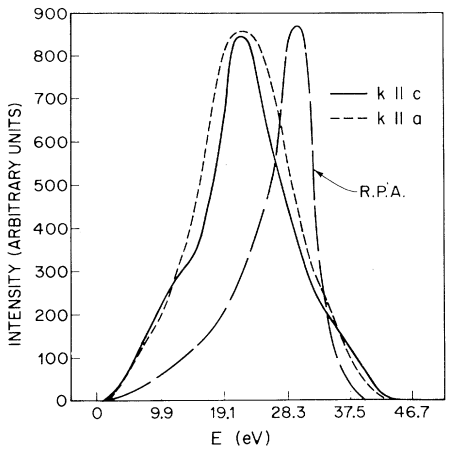

FIG. 3. $K\alpha_1$ spectra obtain for $\theta = 22°$ $\vec{k} \parallel C$ and $\vec{k} \parallel A$ after the $K\alpha_2$ contribution has been subtracted. They are compared with the RPA result which has been smeared with the instrumental resolution function.

turn look different from the homogeneous RPA result. While some of the features in this spectrum no doubt depend on the details of the Be band structure, others may very well be signaling a real breakdown of this simple RPA picture.

*Resident visitor from Columbia University, New York, N. Y. 10027.

[1]H. Watanabe, J. Phys. Soc. Jap. 11, 112 (1956).
[2]C. J. Powell, Proc. Phys. Soc., London 76, 593 (1960).
[3]G. Priftis, Phys. Rev. B 2, 54 (1970).
[4]A. Tanokura, N. Hirota, and T. Suzuki, J. Phys. Soc. Jap. 28, 1382 (1970).
[5]D. M. Miliotis, Phys. Rev. B 3, 701 (1971).
[6]D. Pines and D. Bohm, Phys. Rev. 92, 608 (1953).
[7]P. M. Platzman and P. A. Wolff, *Waves and Interactions in Solid State Plasmas* (Academic, New York, 1973); S. L. Adler, Phys. Rev. 126, 413 (1962); N. Wiser, Phys. Rev. 129, 62 (1963); M. S. Hague and K. L. Kliewer, Phys. Rev. B 7, 2416 (1972).
[8]N. G. Alexandropoulos, J. Phys. Soc. Jap. 31, 1790 (1971).
[9]M. Anderegg, B. Feuerbacher, and B. Fitton, Phys. Rev. Lett. 27, 1565 (1971).
[10]D. F. Dubois and M. G. Kivelson, Phys. Rev. 186, 409 (1969).
[11]A. E. O. Animalu and V. Heine, Phil. Mag. 12, 1249 (1965).
[12]K. L. Kliewer and H. Raether, Phys. Rev. 30, 971 (1973); G. G. Cohen, N. G. Alexandropoulos, and M. Kuriyama, Solid State Commun. 10, 95 (1972).

New Ferroelastic-Ferroelectric Compound: Tanane

D. Bordeaux, J. Bornarel, A. Capiomont, J. Lajzerowicz-Bonneteau, J. Lajzerowicz, and J. F. Legrand
Laboratoire de Spectrométrie Physique, Université Scientifique et Médicale de Grenoble, 38041 Grenoble Cedex, France
(Received 7 May 1973)

We report here evidence for the first paraferroelectric transition observed in a pure molecular solid (without H bonds); we present results from x-ray diffraction, calorimetric and dielectric measurements, and direct optical observation of domain-wall displacement under an applied electric field.

During studies of crystallographic structure of organic free radicals, it has been found that one of these substances, nitroxyde tetramethyl-2, 2, 6, 6-piperidine oxyle ($C_9H_{18}NO$), named Tanane (Fig. 1), has three different phases.[1] In all phases, distances between all neighboring atoms of different molecules are compatible with normal Van der Waals interactions, and, in particular, there is no evidence for intermolecular hydrogen bonding. Two of these phases are connected by a phase change, analogous, from the point of view of symmetry, to that in potassium dihydrogen phosphate (KDP). We present here results showing that this transition is of second order, with a net departure from the mean-field behav-

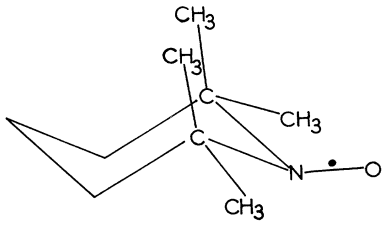

FIG. 1. The Tanane molecule is a saturated heterocycle having a "chair" conformation.